Arab J Sci Eng (2016) 41:2325–2332
DOI 10.1007/s13369-015-1957-6

RESEARCH ARTICLE - EARTH SCIENCES

The Retrieved Urban LST in Beijing Based on TM, HJ-1B and MODIS

Wenfeng Zheng[1] · **Xiaolu Li**[1] · **Lirong Yin**[2] · **Yali Wang**[3]

Received: 19 December 2014 / Accepted: 15 November 2015 / Published online: 14 December 2015

Abstract This paper comparatively analyzed the retrieved land surface temperature (LST) with Landsat Thematic Mapper (TM) sensor and HuanJing (HJ)-1B satellite sensor images using a case study in Beijing, China. The Jmnez-Muoz & Sobrino's (JM&S) single-channel algorithm was applied for retrieving the LST from HJ-1B images. In this study, the temperature measured in the same period under the thermal environmental condition is used to test the precision of temperature product from the Moderate-Resolution Imaging Spectroradiometer (MODIS). The results indicated that: (1) The retrieved LST of three remote sensing data were basically concordant to the measured LST, while the retrieved LST of Landsat TM came closer to the measured data and the other two platforms (MODIS and HJ-1B) were poor compared to the measured data; (2) the retrieved LST of TM, HJ-1B and MODIS was slightly different in the same area, while the distribution and the variation trend of the retrieving LST were consistent; (3) the urban heat island effect of Beijing was particularly obvious, and the vegetation showed a cooling effect. Furthermore, the surface multiplicity type is the main factor influencing the distribution of LST in urban areas. The empirical formulas on the basis of the JM&S single-channel algorithm may need to refit in retrieving LST of HJ-1B.

Keywords Landsat TM · HJ-1B · MODIS · Multisource · Land surface temperature

1 Introduction

Fast urbanization has greatly improved people's life in decades. Meanwhile, it has brought a series of unexpected environmental issues as well. The influence of the urbanization to the urban air temperature is one of the issues [1]. The urban heat environment, especially the urban heat island (UHI), has gradually caused extensive concern in the last decade [2–5]. Land surface temperature (LST) is an important parameter to investigate the earth–atmosphere system dynamics and environment climate [6,7]. As the main monitoring method, thermal infrared remote sensing technology and the methodology to retrieve LST through remote sensing imagery have been well developed [2,8–10]. Based on previous research, the average error of retrieved surface temperature with MODIS was validated to be <1 K or even less [11]. Also the final error of Landsat TM is <1 K [12]. Thermal infrared band function of HJ-1B and Landsat TM have similar curves (Fig. 1). The HJ-1B (10.5–12.5 μm) satellite (launched by China on September 6, 2008) carried CCD cameras, and infrared camera (IRS) is a perfect alternative to Landsat TM as their similar spectral parameters [13–17]. Although lots of efforts have been made in the retrieval research of LST based on single data source, the identity and difference in retrieving LST by multisource have been done by a few researchers [18–20]. In this study, LST retrieved was conducted on the data from three different remote sensing platforms, MODIS, Landsat TM and HJ-1B, and reference

Xiaolu Li and Wenfeng Zheng have contributed equally to this work.

✉ Xiaolu Li
ruth_lee@qq.com; xiaoluli.ruth@gmail.com

[1] School of Automation, University of Electronic Science and Technology of China, Chengdu 610054, China

[2] Geographical and Sustainability Sciences Department, University of Iowa, Iowa City, IA, 52242, USA

[3] School of Foreign Languages, University of Electronic Science and Technology of China, Chengdu, Sichuan, 610054, China

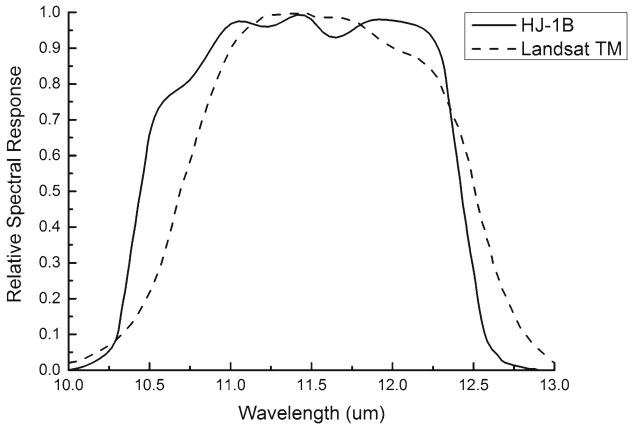

Fig. 1 Thermal infrared band function of HJ and Landsat TM

index was selected with in-situ measured surface temperature data. Retrieved results of different remote sensing platforms were compared and verified, so as to explore the features of different remote sensing platforms data in LST retrieved application.

2 Study Area and Data

The study area is chosen in the urban and suburban area of Beijing (39°54′20″N, 116°25′29′E), the capital of China. It is located in the northwest of the North China Plain. Its west region belongs to Taihang Mountain, and the northern belongs to Yanshan Mountain.

The Landsat TM and HJ-1B images in the study area were obtained on June 8, 2011 (Fig. 2). The MODIS L1B calibrated radiances products and the MODIS temperature products (MOD11A1 land surface temperature/emissivity daily L3 global 1 km) were obtained after half an hour of the same time. Limited by the difference time of passing territory, we chose the TM image data at 10:42 a.m., HJ-1B at 11:03 a.m. and MODIS at 10:30 a.m., which is the closest period among three platforms. It maybe can affect the precision and accuracy of the analysis. Thus, we set the time in June in this study, because the temperature is more stable in the period from 10:30 to 11:00 in summer and sunny days in Beijing, especially on the water body and flagging. It is considered to weaken the affection on the accuracy in this study.

3 Temperature Retrieval Method

According to the channel response function of HJ-1B's thermal infrared band, two typical existing single-channel algorithms—the single-channel algorithm by Qin [18,21] and the universal single-channel algorithm proposed by Jiménezc-Muñoz and Sobrino [8]—were revised by Duan et al. [22]. The two revised algorithms can be applied to the LST retrieval of the HJ-1B thermal infrared band, and the retrieving accuracy of JM&S algorithm is slightly higher than Qin's single-channel algorithm. In this study, JM&S algorithm is used to retrieve LST from Landsat TM and HJ-1B data. The formulations are shown in the reference [8,22,23]. Its parameter sensitivity analysis and accuracy evaluation have been completed using MODTRAN4, an atmospheric radiation transmission software.

It was found that the two revised algorithms can be applied to the LST inversion of the HJ-1B thermal infrared band, and the retrieving accuracy of JM&S algorithm is slightly higher than that of Qin single-channel algorithm. So the paper uses JM&S algorithm to retrieve LST from Landsat TM and HJ-1B image data. Parameters of surface emissivity and atmospheric water vapor content are needed in the single-channel algorithm proposed by JM&S; the retrieving formula is as follows [8]:

$$T_s = \gamma\left[\varepsilon^{-1}\left(\phi_1 L_{\text{sensor}} + \phi_2\right) + \phi_3\right] + \delta \tag{1}$$

$$\delta = -\gamma L_{\text{sensor}} + T_{\text{sensor}} \tag{2}$$

$$\gamma = \frac{C_2 L_{\text{sensor}}}{T_{\text{sensor}}^2}\left[\frac{\lambda^4}{C_1} L_{\text{sensor}} + \lambda^{-1}\right] \tag{3}$$

where T_s is land surface temperature; ε is land surface emissivity; L_{sensor} is radiance at the satellite; T_{sensor} is the corresponding brightness temperature of radiance; λ is effective wave length; $\lambda = 11.457$; $C_1 = 1.19104 \times 10^8\,\text{W}\,\text{cm}^{-2}\,\text{sr}^{-1}\,\mu\text{m}^{-1}$ and $C_2 = 1.43877 \times 10^4\,\mu\text{m}\,\text{K}$ are Planck function constants; ϕ_1, ϕ_2, ϕ_3 are air functions determined by atmospheric water vapor content ω.

Theory of single-channel algorithm is the same, but for different sensors, empirical formula should be refit according to relevant characters of relevant thermal infrared band of the sensors.

In terms of Landsat TM,

$$L_{\text{sensor}} = \frac{\text{DN} \times (L_{\max} - L_{\min})}{255} + L_{\min} \tag{4}$$

where DN is pixel gray value of Landsat TM data, $L_{\min} = 0.1238\ \text{mW}\,\text{cm}^{-2}\,\text{sr}^{-1}\,\mu\text{m}^{-1}$, $L_{\max} = 1.56\ \text{mW}\,\text{cm}^{-2}\,\text{sr}^{-1}\,\text{m}^{-1}$.

In terms of HJ-1B, $L_{\text{sensor}} = \frac{\text{DN}-b}{g}$, g is 60.713, b is −25.441.

Formula retrieving of brightness temperature is as follows:

$$T_{\text{sensor}} = K_2 / \ln(K_1/L_\lambda + 1) \tag{5}$$

In the formula, $K_1 = 2hc^2/\lambda^5$, $K_2 = hc/k\lambda$, $h = 6.626 \times 10^{-34}$ Js, where h is Plank's Constant, c is speed of light, $c = 2.998 \times 10^8\ \text{ms}^{-1}$, $k = 1.380658 \times 10^{-23}\ \text{JK}^{-1}$, and

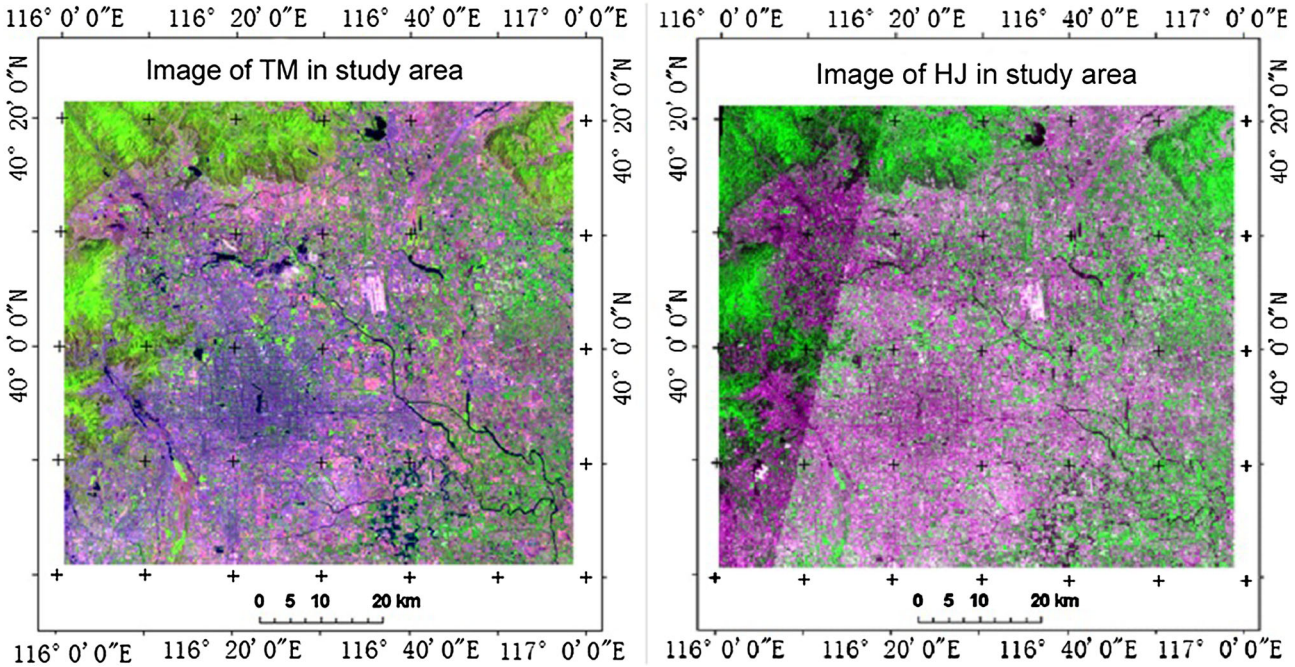

Fig. 2 Image of Landsat TM and HJ-1B in study area

λ is equivalent to center wavelength, $\lambda_{TM} = 11.557$, $\lambda_{HJ} = 11.557$

For Landsat TM thermal infrared band:

Three revised expressions of air function and atmospheric water vapor content proposed by Duan Sibo are as follows [22]:

$$\phi_1 = 0.0412\omega^2 + 0.0936\omega + 0.9856 \quad (6)$$

$$\phi_2 = 0.7174\omega^2 - 0.8812\omega - 0.3941 \quad (7)$$

$$\phi_3 = 0.2639\omega^2 + 0.6499\omega - 0.4703 \quad (8)$$

Water vapor content ω is obtained from MODIS moisture product using the ratio of band 9 and band 2 with a spatial resolution of 1 km:

$$\omega = [(\alpha - \ln(\rho_{19}/\rho_2))/\beta]^2 \quad (9)$$

Surface emissivity ε is estimated by the following which uses Normalized Difference Vegetation Index (NDVI) [22]:

(1) When $0 < \text{NDVI} < 0.05$, $\varepsilon = 0.973$;
(2) When $\text{NDVI} > 0.7$, $\varepsilon = 0.99$;
(3) When $0.05 \leq \text{NDVI} \leq 0.7$, $\varepsilon = 0.04P_v + 0.986$,

$$P_v = [(\text{NDVI} - \text{NDVI}_S)/(\text{NDVI}_V - \text{NDVI}_S)]^2 \quad (10)$$

Two test sites are taken as samples: Tiananmen Square and Peking University. Several urban surface types such as grassland, shrub, rubberized ground, water body, asphalt surface, flagging and asphalt surface under tree are selected as field samples (Fig. 3). The surface temperature measuring instrument we utilized was portable infrared thermometer, with a measurement accuracy of 0.1 °C. The infrared thermometer measured the surface temperature at the vertical height of 10–30 cm. The records were measured hourly by the infrared temperature instrument from local time 7:00–20:00 on June 8, 2011 (Fig. 4). The error of the records is <1 K, and the range of measured values is between −76 and 1832 °F. Each sample was measured five times, and we took the average

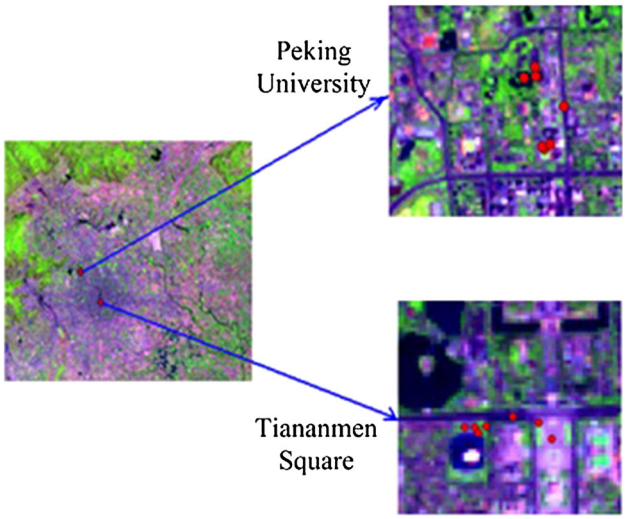

Fig. 3 Distribution of sample points

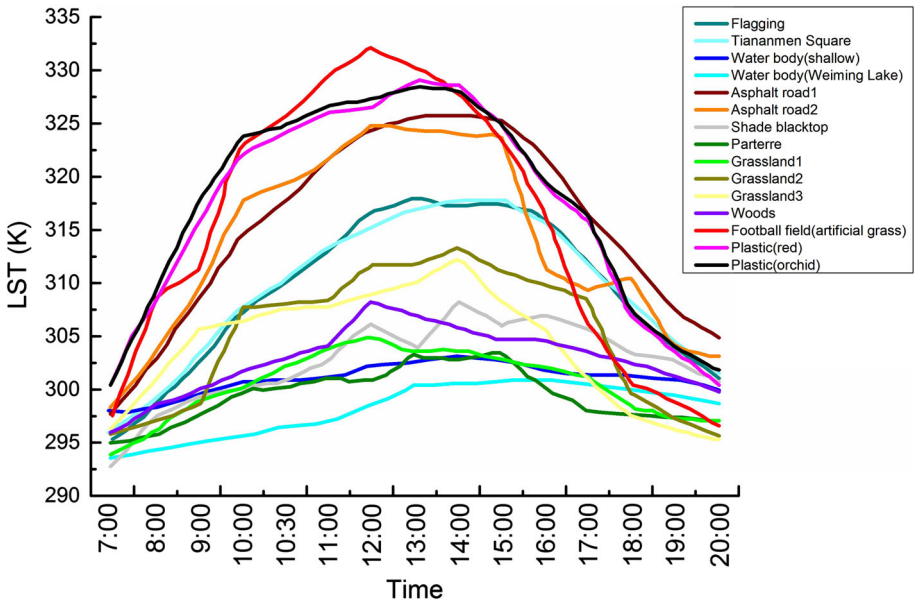

Fig. 4 Temperature of sample points

Table 1 The retrieved LST and the measured value

FID	Land type	Longitude	Latitude	LST (Kevin)				
				Landsat TM	MODIS	Measured (10:30)	HJ-1B	Measured (11:00)
0	Flagging	116.3833	39.90507	307.2	307.9	310.3	303.3	313.1
1	Tiananmen Square	116.3902	39.9026	308.5	307.9	310.4	303.3	313.3
2	Water body (shallow)	116.3846	39.90472	301.4	307.9	296.5	301.9	296.9
3	Water body (Weiming Lake)	116.3043	39.99363	299.6	306.4	300.8	302.8	301
4	Asphalt surface 1	116.3877	39.90584	308.4	307.9	317.7	303.4	321.7
5	Asphalt surface 2	116.3097	39.99079	306.6	307.9	319.4	303.3	321.5
6	Asphalt surface under tree	116.3853	39.90516	304.7	307.9	301	303.4	302.8
7	Parterre	116.3902	39.90543	299.6	306.4	300.3	302.9	301
8	Grassland 1	116.3843	39.90507	305.2	307.9	302.1	303.3	303.8
9	Grassland 2	116.3058	39.99463	303.1	306.4	308	302.9	308.5
10	Grassland 3	116.3071	39.98663	307.2	306.6	307.7	303.7	307.8
11	Shrub	116.3845	39.90507	305.2	307.9	303	303.3	304.1
12	Football field (artificial grass)	116.3059	39.99378	305.6	306.6	325.5	303.7	329.4
13	Rubberized ground (red)	116.3068	39.98685	309.3	306.8	324	302.9	325.9
14	Rubberized ground (orchid)	116.3079	39.98706	309.3	306.4	324.9	302.9	326.6

value as the record. Temperature detectors were calibrated with water temperature.

3.1 Verification Analysis

The overpass time of Landsat TM, HJ-1B and MODIS is 10:42, 11:03 and 10:30, respectively. The measured LST in field samples for verifying the retrieval LST was taken at 10:30 for Landsat TM and MODIS, and at 11:00 for HJ-1B. The measured LST and retrieved values of Landsat TM, HJ-1B and MODIS of each sample points are given in Table 1. The scatter diagram of data is shown in Fig. 5. The retrieved LST of Landsat TM and MODIS is similar and close to measured LST, while the retrieved LST of HJ-1B is largely different from the measured LST. These indicate that retrieving LST by thermal infrared band is feasible.

Parterre, football field, rubberized ground and asphalt surface have large differences between retrieved LST and measured LST, mainly because they are too smaller compared with the satellites' resolution. As Fig. 4 shown, the measured temperature value and change curve are different on the diverse type of urban surface. And the maximum difference of the same land type temperature is up to 30 K in 1 day. Among of all surface types, parterre, football, rubber-

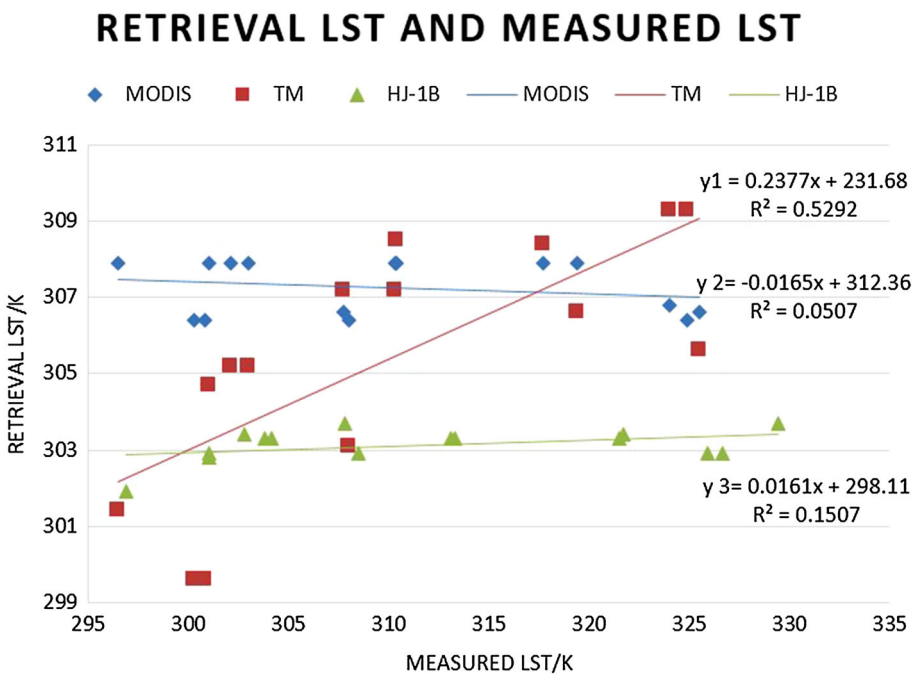

Fig. 5 The scatter diagram on the measured LST and retrieved values

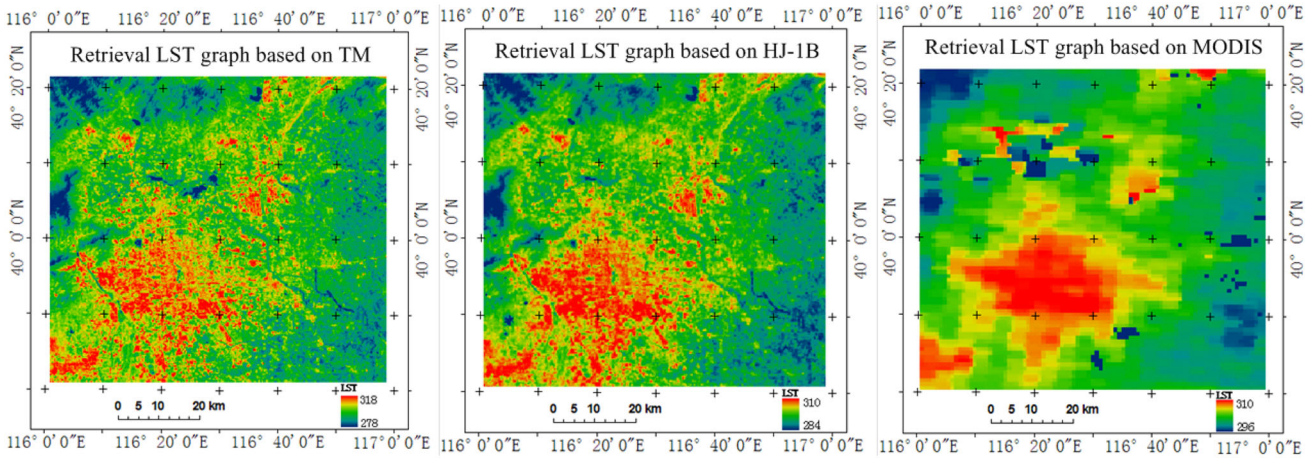

Fig. 6 Retrieval LST graph based on Landsat TM, HJ-1B and MODIS

ized ground and asphalt surface could be more rapidly heated up than any else type. Grasslands 1 and parterre of Tiananmen Square regularly sprayed with water remain a lower LST, which show the great influence from arbor, clouds and moisture.

3.2 Comparative Analysis of Different Sensors

The LST distribution images based on Landsat TM, HJ-1B and MODIS (resolution: 120, 300 and 1000 m, respectively) are shown in Fig. 6. The uncertain ambient noise and the parameter float of the machine lead to slight differences in retrieved LST. But the trend of distribution for retrieval LST is basically consistent. Mixed pixel reduces differences in retrieved LST. For example, retrieval LST of Landsat TM in flagging, Tiananmen Square, water body (shallow) is 307.2, 308.5 and 301.4 K. But for MODIS, these three type lands mixed into one pixel, so its retrieval LST is 307.9 K. With the resolution decreasing from 120 to 1000 m, the trend of the distribution maps of retrieval LST is invariant, but the LST distribution of the specific small land types is hard to be differentiated.

Histograms of retrieval LST of the three sensors are shown in Fig. 7, and the descriptive statistics of retrieved LST are given in Table 2. Retrieval LST of Landsat TM has a wide range (278.3–318.3 K) with maximum and minimum. The retrieval LST of Landsat TM within 301–309 K occupies more than 75 % of the whole area. By contrast, the range of the retrieval LST based on HJ-1B is 284.0–310.1 K. The retrieval LST of HJ-1B within 297–304 K accounts for 95 %

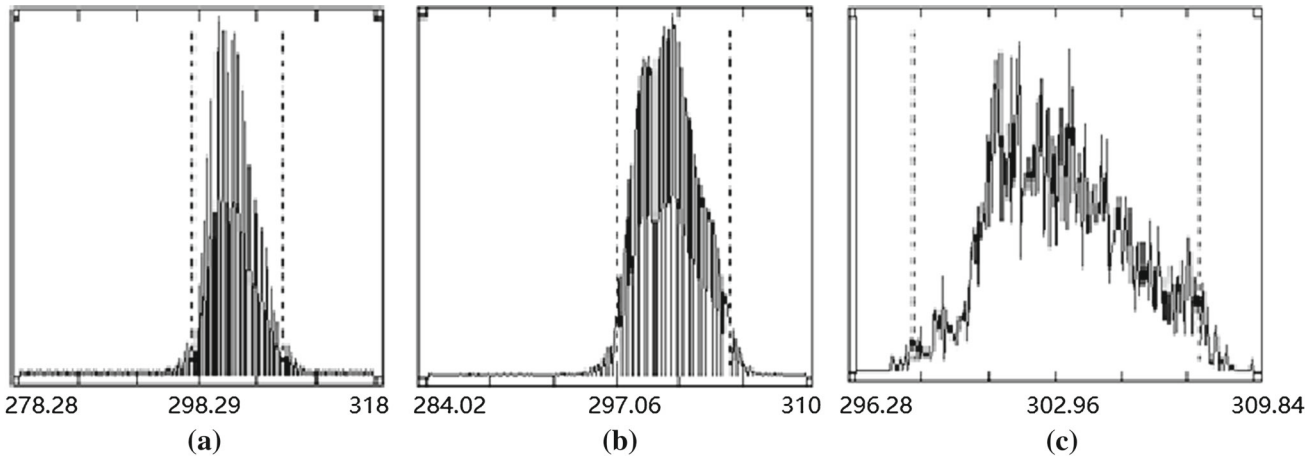

Fig. 7 Histograms of retrieval LST of **a** TM, **b** HJ, **c** MODIS in study area

Table 2 Comparison of retrieval LST based on each sensors

	Maximum	Minimum	Mean value
Landsat TM	318.3	278.3	302.5
HJ-1B	310.1	284	300.8
MODIS	309.6	296.3	303.1

of the whole area. Low resolution of MODIS leads to a narrow range (296.3–309.6 K) of retrieval value. The retrieval LST with MODIS within 300–308 K occupies more than 90 % of the whole area. Obviously, the retrieved LST of HJ-1B is lower than that of Landsat TM and MODIS. According to the scatter diagram on the measured and retrieved LST values in Fig. 5, the slope of the trend line can be used to evaluate the reliability of retrieved LST based on three different remote sensing platforms. It shows that the retrieved LST from Landsat TM image data is high in the highly measured temperature areas. It is most consistent with the change of measured LST in the study area in three remote sensing platforms. However, the retrieved LST from Landsat TM image data has great fluctuation with its trend line. The retrieved LST from HJ-1B is high in the hotter areas as well, but as measured temperatures go up, the retrieved increases much more slowly than Landsat TM. The retrieved LST based on MODIS is a little low in the hotter areas. It maybe is caused by the low spatial resolution of MODIS.

3.3 Analysis of Beijing Thermal Environment Distribution

From the diagram of temperature sample (Fig. 4), it shows that the LST of water body, grassland and shrubs is lower, while the LST of flagging, asphalt surface and football field is higher. For this reason, it can supposedly speculated that LST in urban area is higher than in suburbs. This change curve of temperature in one day clearly indicates that the heat island effect is obvious in urban area. Comparing the distribution map of the retrieved LST (Fig. 6) with the NDVI (Fig. 8) shows that the area with higher LST has lower value in NDVI (in dark color). The areas with high value of NDVI

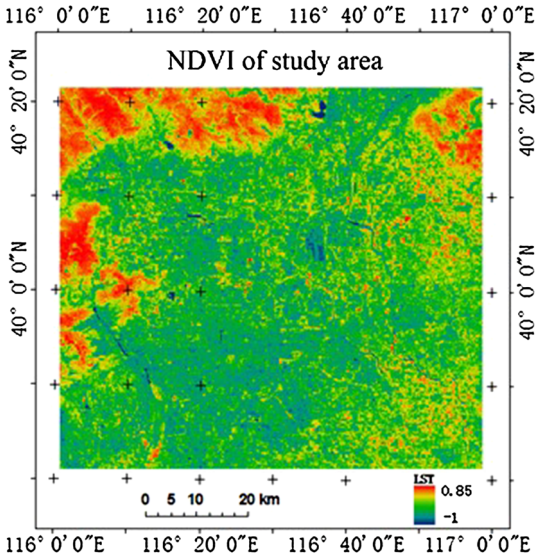

Fig. 8 NDVI of study area

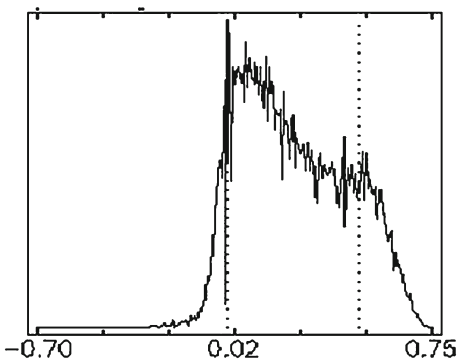

Fig. 9 NDVI distribution curve

are centralized in mountain and forest (Fig. 9). In other words, the LST is correlated negatively with NDVI. Further, it indicates that vegetation maybe has cooling effect on the urban thermal environment.

With the development of urbanization, the original natural vegetation like grassland and farmland has been replaced by artificial buildings such as tarmac and concrete roads. It can lead to the higher urban thermal environment. With the basically stable radiant energy from the sun and the geothermal heating, in the same area the land surface temperature is of extraordinary disparity because of various surface types (Fig. 6). It can show that the land cover affects the amount of energy absorbed by the land surface. Therefore, the urbanization process can be probably greatly influenced on the urban heat island effect.

The LST differences under various land types are large, in which the maximum (artificial grass) reaches to 329.4 K and the minimum (water body) to 296.5 K. It is the asphalt surface whose LST is the highest and changes is the largest. The LST and change of vegetation are lower and smaller, for example grassland 1, grassland 2, grassland 3 and shrubs (Fig. 4). The temperature increases gradually from 7:00, reached the maximum value and changed slightly at 12:00–14:00, and then decreases slowly after 14:00.

4 Conclusion and Discussion

In this study, we have taken the comparative analysis and verification analysis of the retrieved LST based on Landsat TM, HJ-1B and MODIS. The measured LST in Beijing under the same period is set as the reference index. This study focus on comparing the LST retrieved results of the data from three remote sensing platforms. We noticed that resolution of data has effect on retrieved result to some degree. But making transformation on part of the remote sensing data and adopting the rest raw remote sensing data can also decrease the objectivity of the comparative analysis. And different spatial resolution is also one of the features of remote sensing platforms.

The results show that retrieving LST based on thermal infrared band is feasible. The retrieved LST is roughly consistent with the measured data. Landsat TM and MODIS have similar retrieved LST and are close to the measured data. The retrieved LST of HJ-1B is slightly poorer than Landsat TM and MODIS which have more distance to the measured LST. According to Zhao [19] conclusion on the error of retrieved LST based on HJ-1B, the lower LST of HJ-1B is possibly related to the error of moisture estimation and emissivity. From the published data from HJ-1A/B satellite Web site, the calibration coefficients of HJ-1B thermal infrared band are very large. Considering the aging of sensor, spectral response function has slightly changed with passage of time, so the empirical formula for the JM&S single-channel algorithm may need to refit when it is used in retrieving LST of HJ-1B.

The differences in overpass time and resolution lead to the differences of the retrieved LST in the same area, but they have the consistent temperature distribution.

Although there are some differences between the retrieved LST of the Landsat TM, HJ-1B and MODIS, the LST of HJ-1B is accurate with the permitted range of the errors. The HJ satellite could be an ideal alternative free data source for LST retrieval applications.

References

1. Mirzaei, P.A.: Recent challenges in modeling of urban heat island. Sustain. Cities Soc. **19**, 200–206 (2015)
2. Sobrino, J. et al.: Impact of spatial resolution and satellite overpass time on evaluation of the surface urban heat island effects. Remote Sens. Environ. **117**, 50–56 (2012)
3. Stewart, I.D.: A systematic review and scientific critique of methodology in modern urban heat island literature. Int. J. Climatol. **31**(2), 200–217 (2011)
4. Imhoff, M.L. et al.: Remote sensing of the urban heat island effect across biomes in the continental USA. Remote Sens.Environ. **114**(3), 504–513 (2010)
5. Weng, Q.; Lu, D.; Schubring, J.: Estimation of land surface temperature–vegetation abundance relationship for urban heat island studies. Remote Sens. Environ. **89**(4), 467–483 (2004)
6. Emmanuel, R.; Krüger, E.: Urban heat island and its impact on climate change resilience in a shrinking city: the case of Glasgow, UK. Build. Environ. **53**, 137–149 (2012)
7. Jenerette, G.D. et al.: Ecosystem services and urban heat riskscape moderation: water, green spaces, and social inequality in Phoenix, USA. Ecol. Appl. **21**(7), 2637–2651 (2011)
8. Jiménezc-Muñoz, J.C.; Sobrino, J.A.: A generalized single-channel method for retrieving land surface temperature from remote sensing data. J. Geophys. Res.: Atmos. (1984–2012) **108**, D22 (2003)
9. Sobrino, J. et al.: Single-channel and two-channel methods for land surface temperature retrieval from DAIS data and its application to the Barrax site. Int. J. Remote Sens. **25**(1), 215–230 (2004)
10. Sobrino, J.A.; Jiménez-Muñoz, J.C.; Paolini, L.: Land surface temperature retrieval from LANDSAT TM 5. Remote Sens. Environ. **90**(4), 434–440 (2004)
11. Seemann, S.W. et al.: Operational retrieval of atmospheric temperature, moisture, and ozone from MODIS infrared radiances. In: Third International Asia-Pacific Environmental Remote Sensing Remote Sensing of the Atmosphere, Ocean, Environment, and Space. International Society for Optics and Photonics (2003)
12. Padula, F.; Schott, J.: Thermal calibration of landsat 5 TM from 1985 to the present. In: AGU Fall Meeting Abstracts (2008)
13. Chen, P. et al.: Using data of HJ-1A/B satellite for Hulunbeier Grassland aboveground biomass estimation. J. Nat. Resour. **7**, 008 (2010)
14. Sun, L. et al.: Aerosol optical depth retrieval by HJ-1/CCD supported by MODIS surface reflectance data. Sci. China Earth Sci. **53**(1), 74–80 (2010)
15. Huang, H. et al.: Monitoring southwest drought of China using HJ-1A/B and Landsat remote sensing data. In: SPIE Asia-Pacific Remote Sensing. International Society for Optics and Photonics (2012)
16. Chen, J.; Huang, J.; Hu, J.: Mapping rice planting areas in southern China using the China Environment Satellite data. Math. Comput. Model. **54**(3), 1037–1043 (2011)

17. Zhu, H.: Application and evaluation of moonlet datum on environment and calamity monitoring forecast. Arid Environ. Monit. **24**(1), 39–42 (2010)
18. Qin, Z. et al.: Estimating of the essential atmospheric parameters of mono-window algorithm for land surface temperature retrieval from Landsat TM6. Remote Sens. Land Resour. **2**, 37–43 (2003)
19. Zhao, L. et al.: Error analysis of the land surface temperature retrieval using HJ-1B thermal infrared remote sensing data. Spectrosc. Spec. Anal. **30**(12), 3359–3362 (2010)
20. Zhou, J. et al.: A modified single-channel algorithm for land surface temperature retrieval from HJ-1 B satellite data. J. Infrared Millim. Waves **30**(1), 61–67 (2011)
21. Qin, Z. et al.: Landsat TM6 data with calculations of the single-window algorithm for land surface temperature. Acta Geogr. Sonica **56**, 456–466 (2001)
22. Duan, S. et al.: Two single-channel algorithm of retrieving surface temperatures based on HJ-1B simulate analog data. Prog. Nat. Sci. **18**(9), 8 (2008)
23. Li, H. et al.: A single-channel algorithm for land surface temperature retrieval from HJ-1B/IRS data based on a parametric model. In: Geoscience and Remote Sensing Symposium (IGARSS), 2010 IEEE International (2010)